Bulk Organocatalytic Synthetic Access to Statistical Copolyesters from l-Lactide and ϵ-Caprolactone Using Benzoic Acid

Leila Mezzasalma, Simon Harrisson, Saad Saba, Pascal Loyer, Olivier Coulembier, Daniel Taton

Bulk Organocatalytic Synthetic Access to Statistical Copolyesters from *L*-Lactide and ε-Caprolactone Using Benzoic Acid

Leila Mezzasalma,† ‡ Simon Harrisson,§ Saad Saba,‖ Pascal Loyer,‖ Olivier Coulembier,†* Daniel Taton‡**

†Center of Innovation and Research in Materials and Polymers (CIRMAP), Laboratory of Polymeric and Composites Materials, University of Mons, 23 Place du Parc, Mons B-7000, Belgium

‡Laboratoire de Chimie des Polymères Organiques (LCPO), CNRS, ENSCBP University of Bordeaux, UMR 5629, 16, av. Pey Berland 33607 Pessac CEDEX, France

§Laboratoire des IMRCP, Université de Toulouse, CNRS UMR 5623, Université Paul Sabatier, 118 route de Narbonne 31062, Toulouse Cedex 9, France

‖Inserm, INRA, Univ Rennes, Institut NUMECAN (Nutrition Metabolisms and Cancer) UMR-A 1341, UMR S 1241, F-35000 Rennes, France

KEYWORDS: organocatalysis, benzoic acid, lactide, caprolactone, copolymerization, bulk, statistical copolymers.

ABSTRACT

The development of synthetic strategies to produce statistical copolymers based on *L*-lactide (*L*-LA) and ε-caprolactone (CL), denoted as P(LA-*stat*-CL), remains highly challenging in polymer chemistry. This is due to the differing reactivity of the two monomers during their ring-opening copolymerization (RO*c*P). Yet, P(LA-*stat*-CL) materials are highly sought-after as they combine the properties of both polylactide PLA and poly(ε-caprolactone) (PCL). Here, benzoic acid (BA), a naturally occurring, cheap, readily recyclable and thermally stable weak acid, is shown to trigger the organocatalyzed ring-opening copolymerization (ORO*c*P) of *L*-LA and CL under solvent-free conditions at 155 °C, in presence of various alcohols as initiators, with good control over molar masses and dispersities ($1.11 < Đ < 1.35$) of the resulting copolyesters. Various compositions can be achieved, and the formation of statistical compounds is shown through characterization by ^{1}H, ^{13}C and DOSY-NMR spectroscopies and by DSC, as well as through the determination of reactivity ratios ($r_{LA} = 0.86$, $r_{CL} = 0.86$), using the visualization of the sum of squared residuals space method. Furthermore, this BA-ORO*c*P process can be exploited to access metal-free PLA-*b*-P(LA-*stat*-CL)-*b*-PLA triblock copolymers, using a diol as initiator. Finally, residual traces of BA remaining in P(LA-*stat*-CL) copolymers (< 0.125 mol%) do not show any cytotoxicity towards hepatocyte-like HepaRG cells, demonstrating the safety of this organic catalyst.

INTRODUCTION

As biodegradable, nontoxic and biocompatible polymers, polylactide (PLA) and poly(ε-caprolactone) (PCL) can be attractive biosourced surrogates for petroleum-based polymers.[1-4] Both PLA and PCL have been intensively investigated in applications ranging from pharmaceutics to packaging and electronics.[4-7] Yet, both PLA and PCL show some limitations in these applications. For instance, PLA is brittle, exhibits a poor elasticity,[8] a low thermal stability and a modest permeability to drugs. PCL has higher thermal stability and elasticity than PLA, with a glass transition temperature (T_g) around -60 °C *vs.* 45 - 65 °C for PLA,[9,3,10] but suffers from poor mechanical properties. PCL has also a higher permeability to drugs[11]and a half time *in vivo* of 1year,[12] *vs.* a few weeks for PLA.[13] As a result, statistical copolymers of lactide (LA) and ε-caprolactone (CL), *i.e.* P(LA-*stat*-CL) aliphatic copolyesters, are highly sought-after materials as they combine the strengths and minimize the weaknesses of both homopolymers. P(LA-*stat*-CL)s have thus attracted a great deal of attention in the biomedical and pharmaceutical fields,[14-18] and as compatibilizers for PLA/PCL blends.[19] The precision synthesis of P(LA-*stat*-CL) copolymers is still particularly challenging whether organometallic[20] or organic[21-30] catalysts are used. This is due to the highly differing reactivity of the two monomers during ring-opening copolymerization (RO*c*P). LA is typically incorporated first, although CL gives faster rates than LA in homopolymerization reactions.[21-25,27-29,31-37] Aluminum-based catalysts are most efficient for the statistical and controlled RO*c*P of LA and CL,[35,38-40] thought less toxic catalysts based on zinc[41] and molybdenum[42] have also been successfully employed for this purpose.

Organic catalysis for polymerization is a fast developing field in polymer chemistry, offering a number of advantages over metal-catalysis, such as more sustainable processes, reduced toxicity and cost, and easier catalyst synthesis, purification, handling andstorage.[43,44] In this regard, the organocatalyzed ring-opening polymerization (OROP) of LA and CL has been particularly

investigated.[44-50] Attempts to design P(LA-*stat*-CL) copolymers by ORO*c*P, however, have met with limited success.[21-29] Basic-type organocatalysts, such as phosphazenes,[22] *N*-heterocyclic carbenes,[23,27] 1,5,7-triazabicyclo[4.4.0]dec-5-ene guanidine[21] and thiourea-amine[28] only enable incorporation of LA in the polymer chain, and P(LA-*stat*-CL) copolymer synthesis cannot be achieved in this way. In contrast, a few Brønsted acid-type catalysts have been shown to perform the statistical ORO*c*P of LA and CL.[24,25,29] Trifluoromethanesulfonic acid (TfOH) has been used in dichloromethane at 35 °C, providing a preferential insertion of LA units in copolymer chains.[24,25] We have reported the use of dibenzoylmethane, a naturally occurring β-diketone, for the ORO*c*P of *L*-lactide (*L*-LA) and CL in bulk at 155 °C, forming gradient to statistical–like copolymers.[29] In a recent addition, we have described that benzoic acid (BA), another naturally occurring organocatalyst that is also cheap, thermally stable[51] and a readily recyclable weak carboxylic acid, can serve for the metal-free synthesis of polyesters based on PLA and PCL.[52] BA thus allows achieving well-defined PLA and PCL by OROP in bulk, in a temperature range of 155-180 °C, in presence of alcohols as initiators. A bifunctional mechanism where the catalyst would act as a proton shuttle between the monomer and the initiator/chain ends has been postulated. We have also described one example of a P(LA-*stat*-CL) copolymer synthesis by BA-ORO*c*P carried out in bulk.[52]

In the present contribution, we provide a complete description of the P(LA-*stat*-CL) copolymer synthesis in solvent-free conditions. In particular, reactivity ratios of co-monomers have been determined, using both the Kelen-Tüdős linear method and a nonlinear method referred to as "the visualization of the sum of squared residuals space" (VSSRS).[53,54] The P(LA-*stat*-CL) statistical copolymers are characterized by combined analyses, including ^{1}H, ^{13}C and DOSY NMR,

DSC and SEC. The controlled character of this BA-ORO*c*P process is further exploited to achieve PLA-*b*-P(LA-*stat*-CL)-*b*-PLA triblock copolymers, by sequential RO*c*P-mediated synthesis.

EXPERIMENTAL PART

Materials. *L*-Lactide (*L*-LA, 98%, TCI) was recrystallized three times from toluene and dried under vacuum for two days. ε-Caprolactone (CL, 99%, ACROS), butane-1,4-diol (BD, 99%, VWR), and heptan-1-ol (HeptOH, 98%, Sigma Aldrich) were dried over CaH_2 for 48 hours prior to distillation under reduced pressure and were stored on molecular sieves. Methoxypoly(ethylene glycol) ($mPEG_{1000}$, TCI, $M_n \sim 1000$ g.mol^{-1}) was dried by three azeotropic distillations using tetrahydrofuran (THF). Benzoic acid (BA, 99%, ACROS) was recrystallized once and dried by two azeotropic distillations using toluene. Compounds were stored in a glove box ($O_2 \leq 6$ ppm, $H_2O \leq 0.5$ ppm). THF and toluene were dried using an SPS from Innovative technology, stored over sodium benzophenone and polystyrylithium respectively and distilled prior to use.

Methods. NMR spectra were recorded on a Bruker Avance 400 (^1H,^{13}C, 400.2 MHz and 100.6 MHz, respectively) in $CDCl_3$ at 298K.Quantitative ^{13}C NMR was performed on copolymer sample (60 mg in 0.6 mL) using the "INVGATE" sequence with a pulse width of 30°, an acquisition time of 0.7 s, a delay of 4s between pulses and 6144scans in order to investigate the co-monomer distribution within copolymers.[32] Diffusion Ordered Spectroscopy (DOSY)[55,56] measurements were performed at 298K on a Bruker Avance III 400 spectrometer operating at 400.33 MHz and equipped with a 5mm Bruker multinuclear z-gradient direct cryoprobe-head capable of producing gradients in the z direction with strength 53.5 G cm^{-1}. The sample was dissolved in 0.4 mL of $CDCl_3$for internal lock and spinning was used to minimize convection effects. The sample was

thermostated at 298 K for at least 5 minutes before data accumulation. The DOSY spectra were acquired with the *ledbpgp2s* pulse program from Bruker topspin software. The duration of the pulse gradients and the diffusion time were adjusted in order to obtain full attenuation of the signals at 95 % of maximum gradient strength. The values were 2.4 ms for the duration of the gradient pulses and 100 ms for the diffusion time. The gradients strength was linearly incremented in 16 steps from 5% to 95% of the maximum gradient strength. A delay of 5 s between echoes was used. The data were processed using 8192 points in the F2 dimension and 128 points in the F1 dimension with the Bruker topspin software. Field gradient calibration was accomplished at 25°C using the self-diffusion coefficient of H_2O+D_2O of19.0 x 10^{-10} $m^2.s^{-1}$.[57,58]

Molar masses were determined by size exclusion chromatography (SEC) in THF (1mL.min^{-1}) with trichlorobenzene as a flow marker at 313K, using refractometric (RI) detector. Analyses were performed using a three-column TSK gel TOSOH (G4000, G3000, G2000). The SEC device was calibrated using linear polystyrene (PS) standards.

Differential scanning calorimetry (DSC) measurements were carried out with a DSC Q100 LN2 apparatus from TA Instruments under helium flow. The PCL sample was heated for the first run from -130 to 100°C, then cooled again to -130°C and heated again for the third run to 100°C (heating and cooling rate 10°C/min). While PLA sample undergoes 3 runs between -40°C and 200°C and P(LA-*co*-CL) between -70 to 200°C. Glass transition temperatures (T_g) and melting temperatures (T_m) were measured from the second and first heating run, respectively.

General procedure for statistical copolymerization of *L*-LA and CL in presence of BA. In a glove box, previously flamed 10 mL Schlenks were charged with the appropriate amount of *L*-LA and CL, the BA catalyst (2.5, 5 and 10 mol.% relatively to the monomer) and a stir bar. The initiator (BD or HeptOH) was added *via* a 5 or 10 µL syringe while $mPEG_{1000}$ was charged directly in the

Schlenk. The Schlenks were sealed before being introduced in an oil bath preheated at the desired temperature (155-180°C). At specified times, one Schlenk was removed from the oil bath to monitor the reaction by ^{1}H NMR. The as-obtained copolymers were purified by applying vacuum (0.1-0.2 mbars) to the Schlenk at 155°C with a high stirring rate (800-1000 rpm) for 5 minutes. The number average molar mass ($M_{n,SEC}$) and the dispersity ($Đ$) were determined by SEC.

General procedure for triblock synthesis. In a glove box, a previously flamed 10 mL Schlenk was charged with *L*-LA (0.200 g; 1.4 mmol) and CL (0.158 g, 1.4mmol), the BA catalyst (5mol%rel.to monomers) and a stir bar. The BD initiator ($DP_{,th}$= 25 for each monomer) was added *via* a 10 µL syringe. The Schlenk was then sealed before being introduced in an oil bath preheated at 155°C. After 20h of reaction, the Schlenk was introduced in the glove box in order to estimate the monomer conversion *via* ^{1}H NMR spectroscopy and to determine the average molar mass (M_n) and the dispersity ($Đ$) by SEC. The as-obtained copolymer was purified by applying vacuum at 155°C with a high stirring rate. The Schlenk was again introduced into the glove box in order to add more BA catalyst (5mol%rel. to *L*-LA) and the *L*-LA monomer (0.200 g; 1.4 mmol) to target $DP_{,th}\approx$ 25. The polymerization could be restarted by immersing the Schlenk in the oil bath for 25 hours. A sample was collected to estimate conversion by ^{1}H NMR spectroscopy prior to the purification. The as-obtained triblock copolymer was analyzed by SEC, ^{1}H NMR and ^{13}C NMR spectroscopy, DSC and TGA.

Toxicity of BA catalyst. Cytotoxicity was assessed using progenitor and differentiated HepaRG cells incubated for 48 h with various concentrations of BA ranging from 1 to 300 µM**.** HepaRG cells were seeded at a density of 2.6×10^4 cells/cm^2 and cultured in William's E medium supplemented with 10% fetal bovine serum (FBS), 100 units/ml penicillin, 100 µg/ml streptomycin, 2 mM glutamine, 5 µg/ml insulin, and 50 µM hydrocortisone hemisuccinate. After

2 weeks, cell differentiation was further enhanced by maintaining the cells in the same medium supplemented with 2% dimethyl sulfoxide (DMSO) for 2 more weeks. Cell viability was evaluated in progenitor and differentiated cell cultures at day 2 and 30 after plating, respectively, by measuring the intracellular adenosine triphosphate (ATP) content using the CellTiter-Glo® Luminescent Cell Viability Assay (Promega, Charbonnières, France) according to the manufacturer's instructions. Briefly, untreated and treated HepaRG cells were first incubated with the CellTiter-Glo® reagent for 10 min at 37°C. Cells were then transferred in opaque-walled 96-well plates and the luminescent signal was quantified at 540 nm with the POLARstar® Omega microplate reader (BMG Labtech). ATP levels in treated cells were expressed as the percentage of the ATP content measured in untreated cells.

RESULTS AND DISCUSSION

Investigations into the BA-ORO*c*P of *L*-LA and CL in bulk. BA was used to catalyze the RO*c*P of *L*-LA and CL in bulk at 155°C in the presence of butane-1,4-diol (BD), heptanol (HeptOH) and methoxypoly(ethylene glycol) ($mPEG_{1000}$) as initiators. Scheme 1 shows the general synthesis method and Table 1 summarizes the main results obtained. A first series of copolymerization experiments employed different BA catalyst loadings and BD as initiator, with an initial monomer-to-initiator ratio $[L\text{-LA}]_0$:$[CL]_0$:$[I]_0$of 25:25:1 (Table 1, runs 1-4). While the reaction proved sluggish in the absence of BA, with *L*-LA being inserted preferentially (Table 1, run 1), the copolymerization kinetics could be appreciably enhanced by increasing the BA loading from 2.5 to 10 mol% relative to the monomers, confirming the catalytic role of BA (runs 2-4). A catalyst loading of 5 mol% relative to the monomers was selected for the rest of the study, as both

monomers were consumed at the same rate. The initial co-monomer feed ratio ($f_{CL,0}$ = 0.2, 0.3, 0.5, 0.7, 0.9) was then varied, while maintaining a co-monomer-to-initiator ratio of 50 (runs 3, 5-8). In all cases, well-defined and transparent α,ω-bishydroxy-P(LA-*co*-CL) copolymers were obtained (FigureS1, Picture S1). Experimental degrees of polymerizations ($DP_{,exp}$) were consistent with theoretical values ($DP_{,th}$, Table 1) and molar masses ($M_{n,SEC}$) increased linearly with the overall conversion of the monomers (C_{TOT}, Figures1a, S2 and S3). Monomodal and symmetrical SEC traces were observed with dispersity remaining low (1.11 < $Đ$ < 1.25; Figures 1a-b and S2-S4) confirming the good control over the ORO*c*P process. Similar results were obtained using a co-monomer-to-initiator ratio equal to 100 (Table 1, run 9, Figures 1a,c), though a slight discrepancy between $DP_{,exp}$ and $DP_{,th}$ was noted in this case, probably due to side initiation by traces of water.

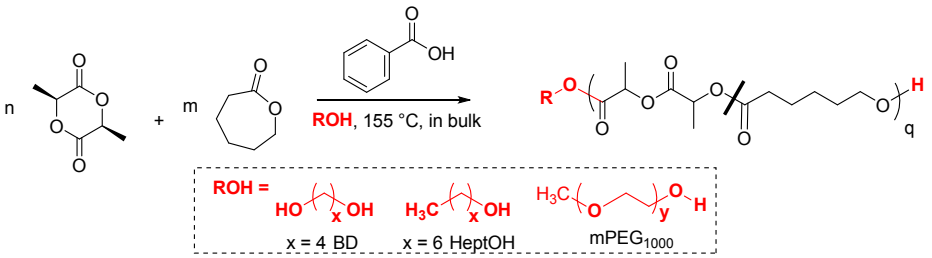

Scheme 1. BA-ORO*c*P of *L*-LA and CL

Table 1. BA-ORO*c*P of *L*-LA and CL in bulkat 155 °C in presence of alcohols as initiators (I).[a]

Run	I	$f_{CL,0}$ (%)[b]	BA (mol%)[c]	Time (h)	C_{CL}/C_{LA} (%/%)[d]	F_{CL} (%)[e]	$M_{n,SEC}$ (g.mol^{-1})[f]	$Đ$[f]	$DP_{,th}$[g]	$DP_{,exp}$[h]
1	BD	51	0	54	15/39	29	2830	1.13	13.4	12.1
2	BD	51	2.5	48	85/91	49	7640	1.18	44.2	42.7

3	BD	51	5	36	85/87	50	7740	1.15	43	42.0
4	BD	52	10	27	92/88	53	8110	1.17	45.1	41.0
5	BD	91	5	7.2	82/78	92	7600	1.25	39.9	39.9
6	BD	72	5	20.5	84/85	71	7140	1.2	42.3	38.0
7	BD	31	5	48	82/80	32	7530	1.11	40.6	38.5
8	BD	21	5	66	86/82	22	8040	1.13	42.1	39.1
9[i]	BD	51	5	73.6	85/83	52	13820	1.25	83	70.0
10	HeptOH	52	5	54	87/92	51	8610	1.35	44.8	41.8
11	PEG	94	5	24	92/89	94	8790	1.58	45.2	n.a

[a]Reactions were performed in bulk at 155°C under argon atmosphere with reaction conditions: $n_{CL} + n_{LA} = 2.8$ mmol; and $[M]_0/[I]_0 = 50/1$ with $[M]_0 = [L\text{-LA}]_0 + [CL]_0$; [b]CL fraction in the initial feed;[c]mol.% of catalyst loading relative to the monomers; [d]CL and *L*-LA conversions were determined by ^{1}H NMR analysis; [e]CL fraction in the pure copolymer; [f]uncorrected average molar mass and dispersity (*Đ*) of crude copolymers determined by SEC chromatography (polystyrene standards) at 40°C and THF as eluent; [g]theoretical degree of polymerization $\boldsymbol{DP_{,th}} = \frac{[L-\boldsymbol{LA}]_0}{[\boldsymbol{I}]_0} \times \boldsymbol{C_{LA}} + \frac{[\boldsymbol{CL}]_0}{[\boldsymbol{I}]_0} \times \boldsymbol{C_{CL}}$; [h]degree of polymerization calculated from the chain ends determined by ^{1}H NMR; [i]$[M]_0/[I]_0 = 100/1$. n.a: not available.

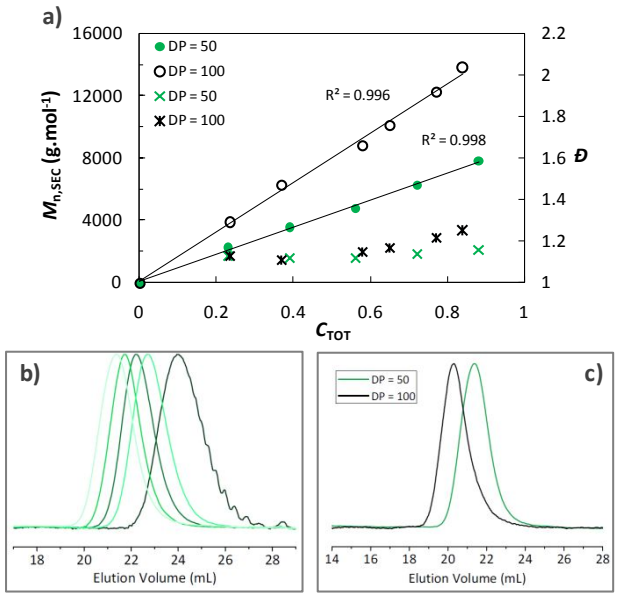

Figure 1.(a) Evolution of uncorrected $M_{n,SEC}$ (•) and dispersity $Đ$ (x) with total monomer conversion (C_{TOT}); (b) evolution of SEC molar masses with time (conditions corresponding to run 3, Table 1); (c) SEC comparison of runs 3 and 9 (Table 1).

As BA organocatalyst remained in the crude copolymers, these were purified to avoid any premature degradation,[21,59] for instance during processing.[60] For this purpose, we exploited the capability of BA and *L*-LA to sublimate and of CL to evaporate following a solvent-free and straightforward purification procedure that was set up in our previous study (see experimental part).[52] This also allowed us to recycle and reuse BA for further organocatalytic cycles, leading to chemically pure P(LA-*co*-CL) copolyesters.[52]

Determination of reactivity ratios and analysis of P(LA-*co*-CL) microstructure. Analysis by ^{1}H NMR spectroscopy evidenced that both co-monomers were inserted in the copolymer chain throughout this BA-ORO*c*P process, irrespective of the initial co-monomer feed (Figure 2, Figure S5, Table 1).

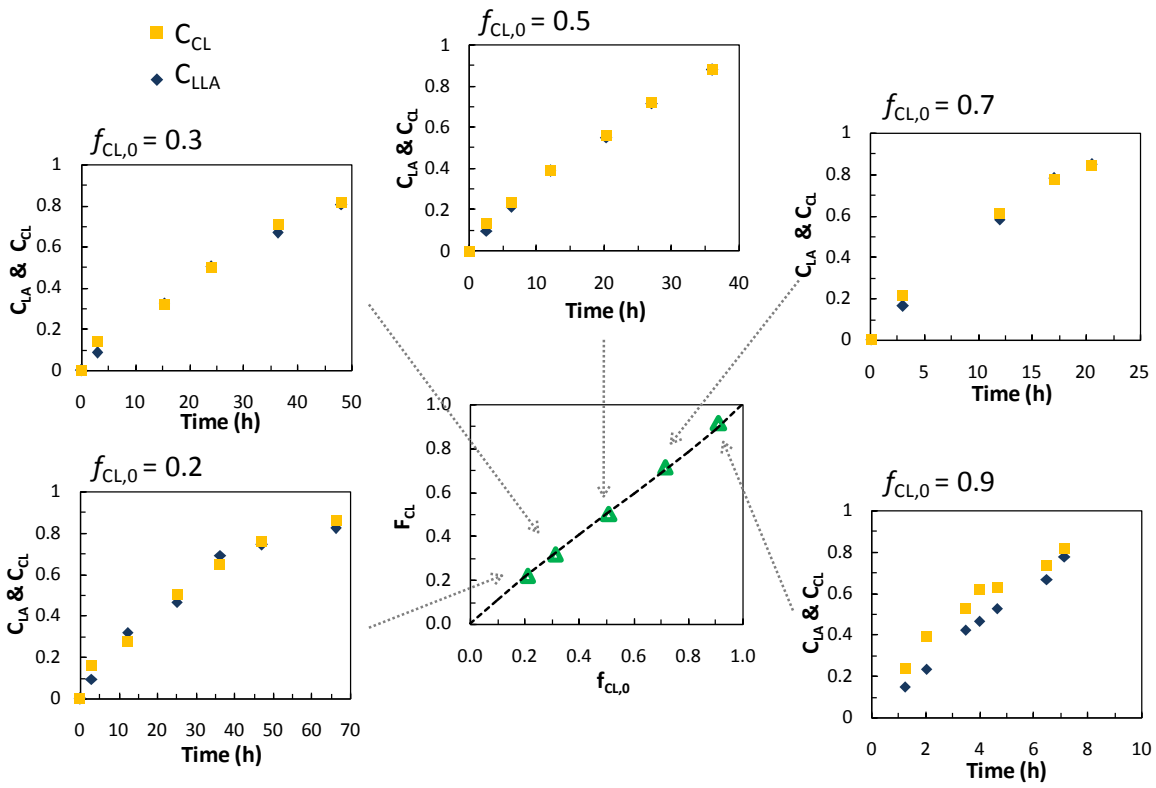

Figure 2. Evolution of the overall monomer conversion *vs.* time for different contents in CL in the initial feed ($f_{CL,0}$ = 0.2, 0.3, 0.5, 0.7, 0.8; runs 3 and 5-8, respectively) and evolution of CL content in the final copolymer (F_{CL}) *vs.* $f_{CL,0}$. Dashed line represents expected F_{CL} for $r_{CL} = r_{LA} = 0.86$ using the Mayo-Lewis equation (**2**).

In order to account of the copolymer microstructure, reactivity ratios of *L*-LA (r_{LA}) and CL (r_{CL}) were evaluated using the Kelen-Tüdős method, for the BA-ORO*c*P of *L*-LA and CL carried out in bulk at 155°C (Scheme S1, Figure S6, Table S1). These kinetic investigations led to the following values: $r_{LA} = 0.66$, $r_{CL} = 0.91$. However, linearized methods such as Kelen-Tüdős, which derive from the Mayo-Lewis equation and require that monomer conversion should be kept very low, can distort the error structure of the data and may provide biased estimates of reactivity ratios. This prompted us to implement a less biased method, the "visualization of the sum of squared residuals space" (VSSRS), a nonlinear method[53,54] developed by Van den Brink *et al.* This VSSRS method not only allows for an estimate of the reactivity ratios at high conversion, but also takes into account errors both on the monomer conversion and the co-monomer ratios, thus providing

unbiased estimates of the reactivity ratios as well as joint confidence regions. Data related to monomer conversion, copolymer composition (F) and co-monomer ratio (f) were fitted to the integrated form of the Mayo-Lewis copolymer composition equation, (**1**):

$$\textbf{(1)} \qquad C_{TOT} = 1 - \left(\frac{f_{CL}}{f_{CL,0}}\right)^{\alpha} \times \left(\frac{f_{LA}}{f_{LA,0}}\right)^{\beta} \times \left(\frac{f_{CL,0} - \delta}{f_{CL} - \delta}\right)^{\gamma}$$

$$\alpha = \frac{r_{LA}}{1 - r_{LA}}, \quad \beta = \frac{r_{CL}}{1 - r_{CL}}, \quad \gamma = \frac{1 - r_{CL} \times r_{LA}}{(1 - r_{CL}) \times (1 - r_{LA})}, \quad \delta = \frac{1 - r_{LA}}{2 - r_{CL} - r_{LA}}$$

The reactivity ratios were found equal to $r_{CL} \approx r_{LA} \approx 0.86$. Figure 3a shows the point estimates and the confidence regions obtained using theVSSRS method. The 95% confidence intervals were almost the same for both r_{CL} (0.74 – 1.01) and r_{LA} (0.75 – 1.00).

Theoretical plots of f_{CL} and F_{CL} as a function of C_{TOT} were then modeled from values of the reactivity ratios obtained by the VSSRS method (Figures 3 b&c, solid lines). These plots fit well the experimental data obtained in the course of the bulk BA-ORO*c*P of *L*-LA and CL at 155°C (Figures 3 b&c, black dots). When plotting $F_{CL,th} = g(f_{CL,0})$ from the reactivity ratios obtained by the VSSRS method (Figure 2, dashed line) using the Mayo-Lewis equation (**2**),[61] we observed a total agreement with experimental data ($F_{CL,exp} = g(f_{CL,0})$, Figure 2). The overall composition F_{CL} was also found in full accordance with co-monomer contents used in the feed ratio throughout the whole ORO*c*P process. The slight deviation observed at conversion lower than 20% might be due to uncertainties in the NMR measurements. These deviations at low conversion account for the difference in estimates of reactivity ratios by the Kelen-Tüdős method and the VSSRS method.

$$\textbf{(2)} \qquad F_{CL,th} = \frac{r_{CL} \times f_{CL}^{\,2} + f_{CL} \times f_{LA}}{r_{CL} \times f_{CL}^{\,2} + 2 \times f_{CL} \times f_{LA} + r_{LA} \times f_{LA}^{\,2}}$$

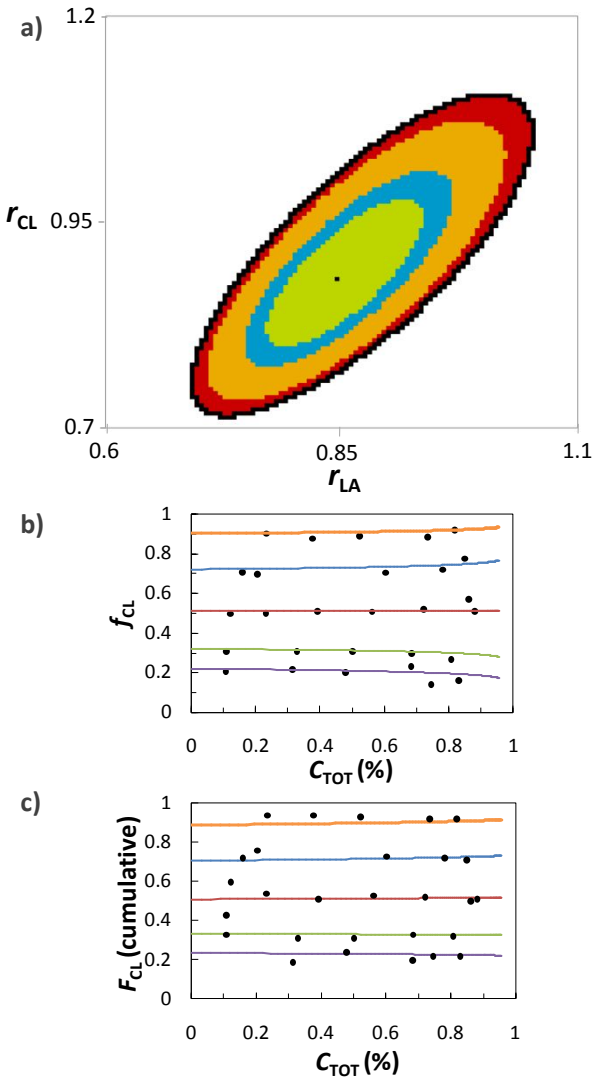

Figure 3.(a) 95% Joint confidence interval (JCI) for reactivity ratios with point estimate (r_{CL}= r_{LA} =0.86). Internal contours indicate 50%, 70%, and 90% JCIs. (b) Prediction of the co-monomer ratio (solid lines) as a function of conversion *vs.* experimental points (black dots). (c) Prediction of the cumulative copolymer composition (solid lines) as a function of conversion versus experimental points (black dots).

These kinetic results strongly support the formation of statistical copolymers when using BA in ORO*c*P of *L*-LA and CL. Copolymer structures were further analyzed by ^{1}H and ^{13}C NMR spectroscopy from various *L*-LA/CL ratios (Table 1, runs 3, 5-8). The ^{1}H NMR spectrum of the copolymer obtained from BA-ORO*c*P involving an equimolar ratio of *L*-LA and CL (Table 1, run 3) showed all representative peaks due to homo- and heterodiads, as illustrated in Figure 4a.

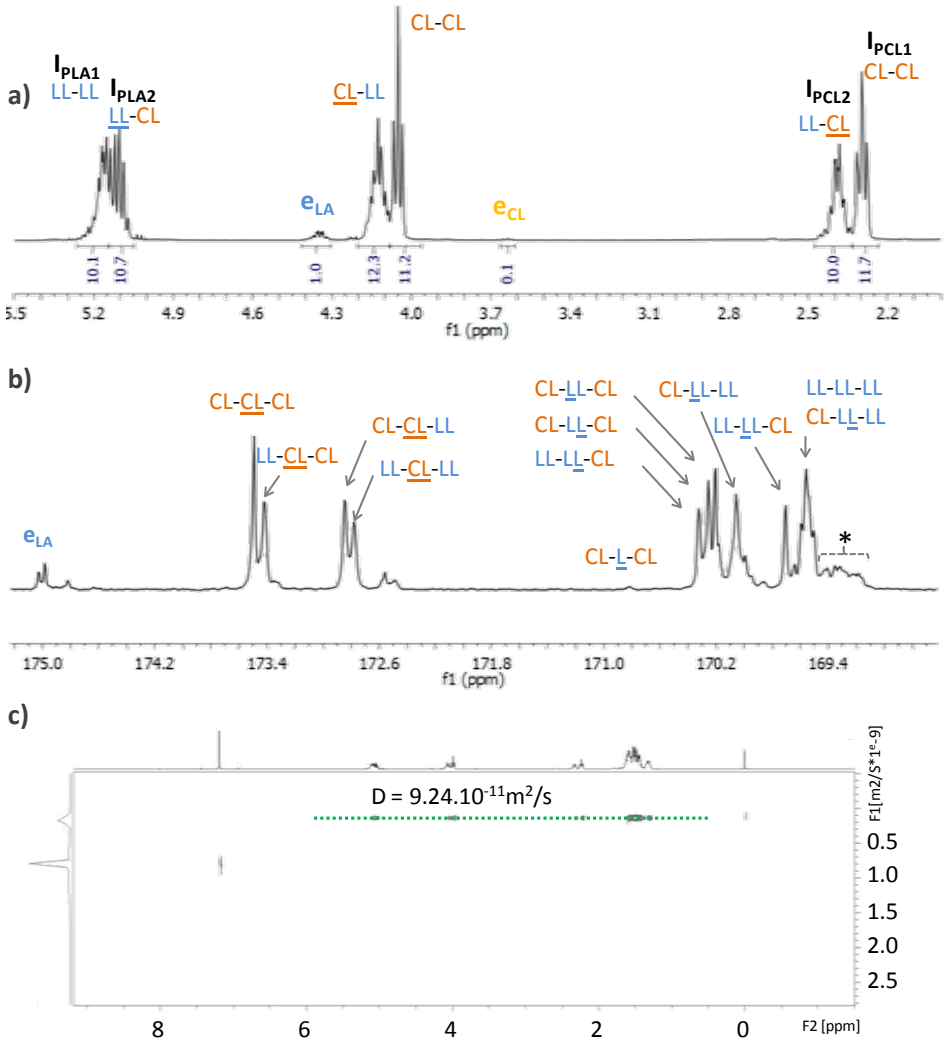

Figure 4. (a)^{1}H (400.2 MHz, r.t.) and (b) ^{13}C (100.6 MHz, r.t.) NMR spectra of a P(LA-*co*-CL) copolymer in $CDCl_3$ (Table 1,run 3); LL and L refer to lactidyl and lactoyl units, respectively; * epimerized LL-LL-LL sequences; (c) DOSY NMR spectrum ($CDCl_3$, 400.2 MHz, r.t) of pure copolymer (Table 1, run 3).

As expected for statistical copolymers, integral values of the homosequences closely matched those of the heterosequences for both PLA (10.1/10.7, δ around 5.1 ppm) and PCL (11.7/10.0, δ around 2.35 ppm). Interestingly, the integral value of the terminal lactidyl units (e_{LA}) appearing at 4.36 ppm was ten times greater than that of the terminal caproyl units (e_{CL}) at 3.62 ppm.This might be explained by the higher reactivity of caproyl units at chain-ends, which after fast crossover gave rise to less reactive terminal lactidyl units. This can only be stated because

reactivity ratios are close to 1 for both monomers ($r_{CL} \approx r_{LA} \approx 0.86$), and because the BA-OROP of CL is 20 times faster than that of *L*-LA ($k_{CL\text{-}CL} >> k_{LA\text{-}LA}$; Scheme S1).[52] In these conditions, one can write the following relationships: $k_{CL\text{-}CL} \approx k_{CL\text{-}LA} >> k_{LA\text{-}LA} \approx k_{LA\text{-}CL}$ using equations (**3**):

$$(\mathbf{3})\ r_{CL} = \frac{k_{CL-CL}}{k_{CL-LA}} \qquad r_{LA} = \frac{k_{LA-LA}}{k_{LA-CL}}$$

Analysis by ^{13}C NMR spectroscopy (Figure 4b) also confirmed the microstructure of the copolymer with the expected homo- and heterotriads, as previously reported.[62] Kasperczyk and Bero described two distinct modes of transesterification reactions during the RO*c*P of LA and CL, as depicted in Scheme 2.[63] Here, the "second mode of transesterification reactions", *i.e.* giving rise to the anomalous CL-L-CL sequences (L representing one lactoyl unit) at 170.8 ppm, was barely observed. As the dispersity of the resulting copolymers remained low (1.11 <*Đ*< 1.25), transesterification reactions — if present — occurred to a minor extent during the bulk BA-ORO*c*P process of *L*-LA and CL at 155°C.

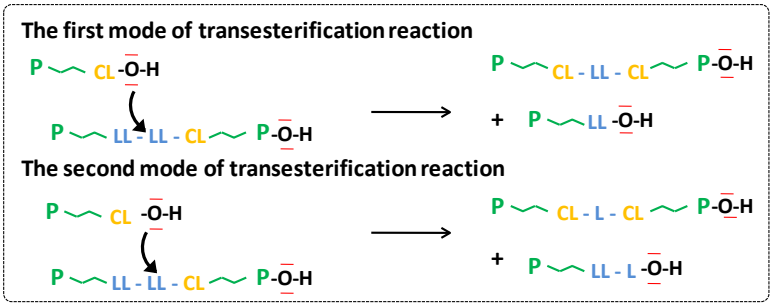

Scheme 2. The two modes of transesterification reactions.

Two series of peaks were also observed at 172.5 ppm and 175 ppm. While after performing HMBC analyses, peaks at 175 ppm could be ascribed to the carbonyl carbon (-C(O)-) of the lactidyl unit at the copolymer chain ends (Figure S7), peaks around 172.5 ppm could not be clearly

attributed, and might be the result of minor side reactions occurring at high temperature. In addition, only one diffusion coefficient was determined by DOSY-NMR ($D = 9.24 \times 10^{-11}$ $m^2.s^{-1}$, $DP_{,exp} = 42$, Figure 4c) that was different from that of PLA ($D = 1.32 \times 10^{-10}$ $m^2.s^{-1}$, $DP_{,exp} = 21$) and of PCL ($D = 5.54 \times 10^{-11}$ $m^2.s^{-1}$; $DP_{,exp} = 21$, Figures S8-S11). The same peaks of homo- and heterosequences, though of different intensities, were observed for copolymers of differing composition (runs 3 and 5-8, Table S2, Figures S12-14). As expected, the content of CL heterodiads, as determined by ^{1}H NMR, decreased linearly with the initial feed in CL (Table S2, Figure S15). The average block length of the caproyl (L_{CL}) and lactidyl (L_{LA}) units could also be assessed by ^{1}H and quantitative ^{13}C NMR analyses and compared with the theoretical values ($L_{CL,th}$ and $L_{LA,th}$) obtained from equations (**4**) (Figures 5& S13, Table S2).

$$(4) \qquad L_{CL,th} = \frac{r_{CL} \times f_{CL} + f_{LA}}{f_{LA}} \quad L_{LA,th} = \frac{r_{LA} \times f_{LA} + f_{CL}}{f_{CL}}$$

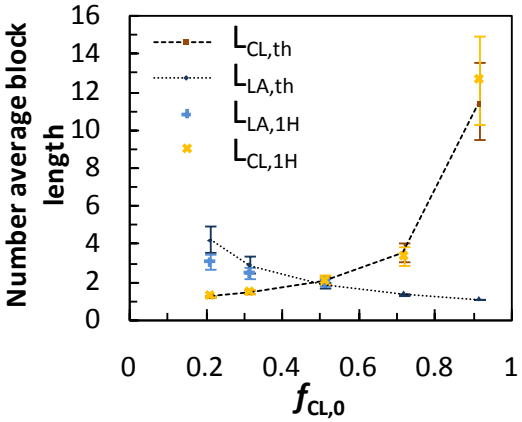

Figure 5. Theoretical number average block lengths ($L_{CL,th}$ and $L_{LA,th}$) as a function of $f_{CL,0}$and experimental average block lengths determined by ^{1}H NMR spectroscopy ($L_{CL,1H}$ and $L_{LA,1H}$) for different $f_{CL,0}$.

For the pure copolymer of F_{CL} = 0.5 (run 3, Table 1), L_{CL} and L_{LA} values determined by ^{13}C NMR ($L_{CL,13C}$ =2.2 and $L_{LA,13C}$= 2.1) were in excellent agreement with the theoretical values ($L_{CL,th}$ = 1.9 and $L_{LA,th}$ = 1.8) and with those determined by ^{1}H NMR spectroscopy ($L_{CL,1H}$ = 2.1 and $L_{LA,1H}$= 1.9). Finally, glass transition temperatures, as determined from the second run of DSC analyses ($T_{g,exp}$), were consistent with values expected from the Fox equation ($T_{g,Fox}$, Figure 6, Table S2 and Figure S16).

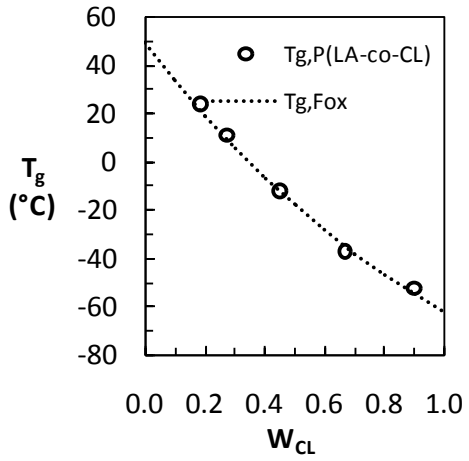

Figure 6. Experimental glass transition temperature of the P(LA-*co*-CL) copolymers as a function of the weight fraction of CL in the copolymer. Dotted line, theoretical glass transition temperature of the copolymers calculated from Fox equation.

Triblock copolymer synthesis and use of other alcohol initiators than BD. Controlled synthesis of P(LA-*stat*-CL) copolyesters prompted us to derive triblock copolymers by sequential BA-ORO*c*P, using BD as initiator. As depicted in Scheme 3, an α,ω-bis-hydroxy P(LA-*stat*-CL) precursor ($M_{n,SEC}$= 5480 g.mol^{-1}, $Đ$ = 1.12) was synthesized first, using the conditions described previously ([*L*-LA]$_0$/[CL]$_0$/[BD]$_0$/[BA]$_0$= 25/25/1/2.5; Table S3). After 20 hours, extra *L*-LA was added at a [*L*-LA]$_0$/[BA]$_0$/[P(LA-*stat*-CL)]$_0$ ratio equal to 25/1.25/1, and the reaction was stirred

for 25 hours at 155°C, reaching a conversion in PLA of 50%. Formation of the PLA-*b*-P(LA-*stat*-CL)-*b*-PLA triblock copolymer was attested by a clear shift in SEC to higher molar mass ($M_{n,SEC}$ = 8450 g.mol^{-1}, $Đ$ = 1.15, Figure 7c, Table S3). Analysis by ^{1}H NMR confirmed the presence of both P(LA-*stat*-CL) and PLA blocks, with representative protons of heterodiads from the statistical central block and increased intensity of PLA homodiads after BA-OROP of *L*-LA (see Figures 7a & b). The proton signals at 3.6 ppm due to hydroxy-methylene PCL end-groups of the copolymer precursor totally vanished (Figure 7a) in favor of the methine end-groups of PLA block at 4.36 ppm (Figure 7b). Furthermore, the experimental degree of polymerization determined by ^{1}H NMR was very close to the theoretical value based on the initial ratio of *L*-LA and P(LA-*stat*-CL). The increased intensity of the LL-LL-LL triads (Figure S17) in^{13}C NMR confirmed the triblock copolymer synthesis. No evidence for the occurrence of transesterification reactions of type II was noted, as anomalous CL-L-CL triads at 170.8 ppm were not observed (Figure S17).

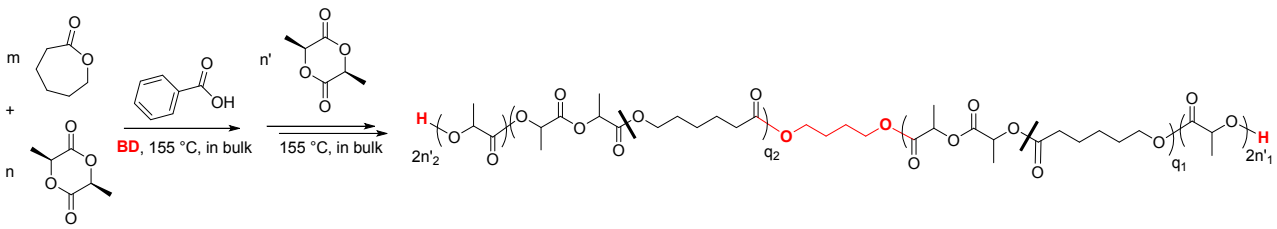

Scheme 3. Synthesis of PLA-*b*-P(LA-*stat*-CL)-*b*-PLA triblock copolymers by sequential BA-ORO*c*P of *L*-LA and CL initiated by BD, followed by a BA-OROP of *L*-LA (q=n + m= $q_1 + q_2$ and $n' = n_1' + n_2'$).

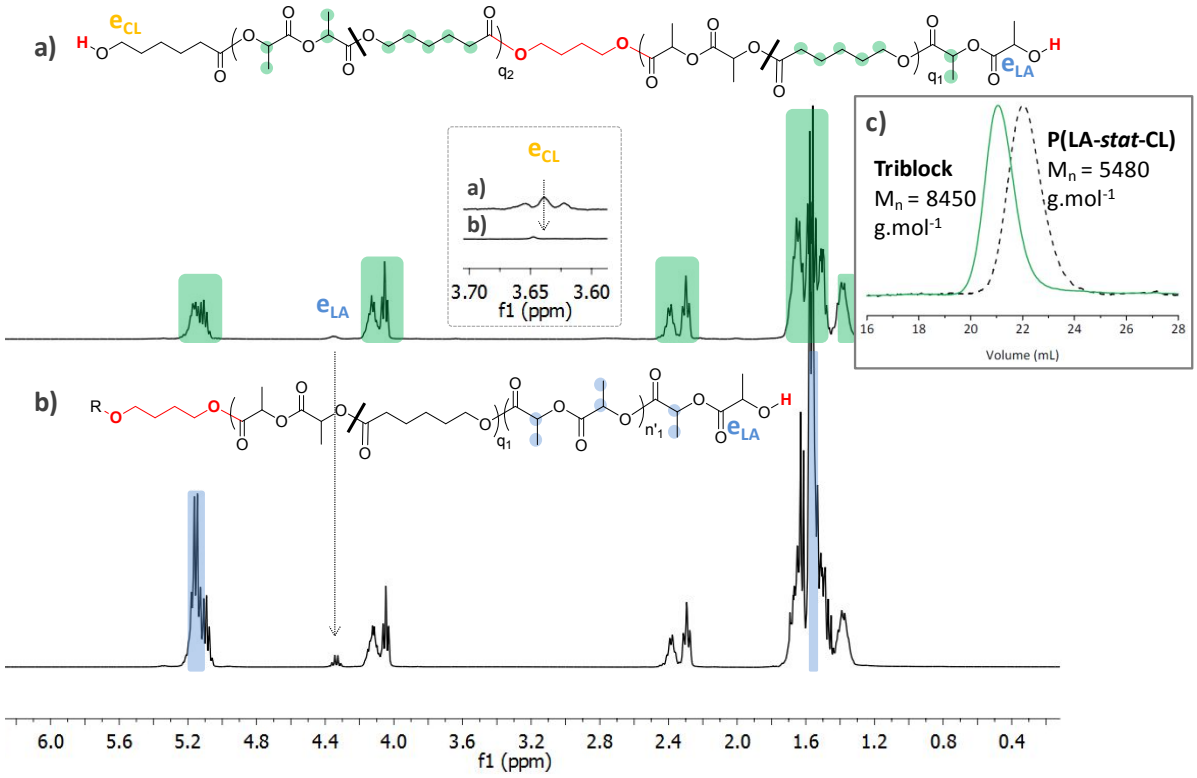

Figure7. ^{1}H NMR spectra of (a) P(LA-*stat*-CL) macroinitiator and (b) PLA-*b*-P(LA-*stat*-CL)-*b*-PLA triblock copolymer ($CDCl_3$, 400MHz, r.t); R represents the second arm of the triblock copolymer; (c) Normalized SEC traces from RI detector of P(LA-*stat*-CL) (black dashed line) and corresponding triblock copolymer ($M_{n,SEC}$ determined by SEC in THF).

To demonstrate the versatility of BA as an organocatalyst, HeptOH and $mPEG_{1000}$ were evaluated as initiators for the bulk ORO*c*P of *L*-LA and CL at 155°C (Table 1, runs 10-11). Well-defined P(LA-*stat*-CL) could be obtained using HeptOH ($[L\text{-LA}]_0/[CL]_0/[HeptOH]_0/[BA]_0$=

25/25/1/2.5), with $M_{n,SEC}$ increasing linearly with $C_{TOT,}$ a theoretical DP in agreement with the experimental one, and monomodal SEC traces with fairly low dispersity ($Đ < 1.35$) for bulk RO*c*P (Figures S19-S20, Table 1, run 10). The overall composition in the copolymer was in agreement with the initial co-monomer ratio ($f_{CL,0} = 0.52$, $F_{CL} = 0.51$). Synthesis of mPEG-*b*-P(LA-*co*-CL) diblock copolymer could also be achieved using commercial $mPEG_{1000}$ as macroinitiator under the same conditions mentioned above. An initial co-monomer composition of $f_{CL,0} = 0.94$ was selected to obtain a semi-crystalline diblock copolymer (Tables 1, run 11, Figures S21 to S23,). Efficient crossover from $mPEG_{1000}$ to the targeted diblock was confirmed by the shift to lower elution volume after polymerization with a monomodal SEC trace ($M_{n,SEC}$ = 8790 g.mol^{-1}, $Đ$ = 1.58; Figure S22).

Study of the cytotoxicity of benzoic acid. Residues of some organocatalysts such as thioureas[43] and phosphazenium salt[64] have been found in synthetic (co)polymers and these catalysts induce significant cytotoxicity. As benzoic acid remained in our copolymers (< 0.125 mol%),[52] it was crucial to study its toxicity. We assessed the cytotoxicity of BA using the human HepaRG hepatoma cells in two culture conditions. These cells are bipotent hepatic progenitors actively proliferating at low cell density, which provides a first experimental condition to assess cytotoxicity on the process of cell division since these cells kept the major cell cycle check points and express wild-type P53, Retinoblastoma and beta-catenin genes.[65] When these cells are cultured at high cell density, they become quiescent and differentiate to generate a co-culture cell model combining cholangiocyte- and hepatocyte-like cells,[66] which is recognized as a suitable alternativemodelto primary culture of human hepatocytes to study hepatic metabolism[67,68] and (geno)toxicity[69,70] of xenobiotics because differentiated HepaRG cells express all transporters and drug-metabolizing enzymes found *in vivo* in the liver. Both progenitor and differentiated cells were

incubated in culture media containing BA in a wide range of concentrations from 1 to 300 µM to assess the effect(s) of BA on proliferating hepatic cells as well as cholangiocyte- and hepatocyte-like cells. Benzoic acid was found to be non-toxic at these concentrations (Figure 8) in these different *in vitro* models of human hepatic cells demonstrating that BA did not trigger adverse effects on cell proliferation and cytotoxicity in metabolically competent hepatic cells.

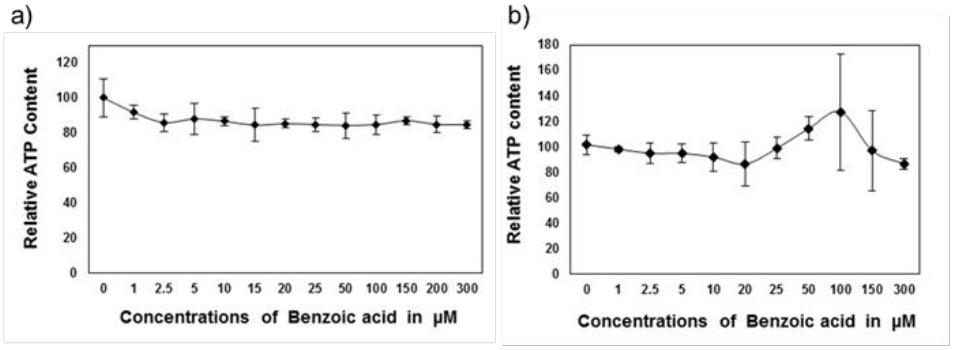

Figure 8. Determination of the relative ATP contents in untreated or treated cultures of progenitor (a) and differentiated cholangiocyte- and hepatocyte-like (b) HepaRGcells. ATP content was arbitrarily set as 100% in untreated cells. No significant alterations of the ATP contents were found in cells treated with benzoic acid at concentrations of 1 to 300 µM.

CONCLUSION

This work addresses a difficult challenge in polymer chemistry, namely, statistical copolymer synthesis based on poly(ε-caprolactone) and poly(L-lactide). Benzoic acid (BA) proves very versatile to this end as it can catalyze the metal-free and statistical ring-opening copolymerization (RO*c*P) of *L*-lactide (*L*-LA) and ε-caprolactone (CL). A library of statistical copolymers of varying *L*-LA/CL compositions can thus be synthesized in bulk at 155°C, in presence of various alcohols as initiators, with a relatively good control over molar masses and dispersities. The statistical character of the copolymers is supported by ^{1}H and ^{13}C NMR analyses

showing homo- and heterosequences and by the glass transition temperatures of the copolymers, that are in good agreement with values calculated from the Fox equation. Moreover, reliable reactivity ratio values of *L*-LA (r_{LA} = 0.86) and CL (r_{CL} = 0.86) have been calculated using "the visualization of the sum of squared residuals space" (VSSRS) method, with a narrow 95% confidence interval for *L*-LA (0.75-1.01) and CL (0.74-1.0). The average block lengths of lactidyl and caproyl units, as determined by ^{1}H NMR and by quantitative ^{13}C NMR spectroscopies, closely match theoretical values. The "controlled/living" character of this BA-catalyzed process is further demonstrated through the synthesis of PLA-*b*-P(LA-*stat*-CL)-*b*-PLA triblock copolymers, using butane-1,4-diol as initiator. This work thus expands the scope of organocatalyzed polymerization reactions, by providing a straightforward and metal-free synthetic alternative to biodegradable, biocompatible and aliphatic statistical copolyesters based on PLA and PCL, thanks to the use of BA as a weakly acidic and non-toxic organocatalyst.

ASSOCIATED CONTENT

Supporting Information. Copolymerization procedure using the different initiators, triblock copolymer synthesis, related NMR spectra and DSC thermograms, determination of reactivity ratios are available free of charge via the Internet at http://pubs.acs.org.

AUTHOR INFORMATION

Corresponding Authors

*E-mail:harrisson@chimie.ups-tlse.fr

*E-mail:olivier.coulembier@umons.ac.be

*E-mail:taton@enscpb.fr

Notes

The authors declare no competing financial interest.

ACKNOWLEDGMENT

This work was supported by the EU Horizon 2020 Research and Innovation Framework Program — European Joint Doctorate—SUSPOL-EJD (grant number 642671), by the European Commission and Region Wallonne FEDER program and OPTI2MAT program of excellence, by the Interuniversity Attraction Pole Programme (P7/05) initiated by the Belgian Science office and by the FNRS-FRFC. This work was also funded by the Institut National de la Santé et de la Recherche Médicale (Inserm, France). O.C. is Research Associate for the F.R.S.-FNRS of Belgium.

REFERENCES

(1) Wedde, S.; Rommelmann, P.; Scherkus, C.; Schmidt, S.; Bornscheuer, U. T.; Liese, A.; Gröger, H. An Alternative Approach towards Poly-ε-Caprolactone through a Chemoenzymatic Synthesis: Combined Hydrogenation, Bio-Oxidations and Polymerization without the Isolation of Intermediates. *Green Chem.* **2017**, *19* (5), 1286–1290. https://doi.org/10.1039/C6GC02529C.

(2) Buntara, T.; Noel, S.; Phua, P. H.; Melián-Cabrera, I.; de Vries, J. G.; Heeres, H. J. Caprolactam from Renewable Resources: Catalytic Conversion of 5-Hydroxymethylfurfural into Caprolactone. *Angew. Chem. Int. Ed.* **2011**, *50* (31), 7083–7087. https://doi.org/10.1002/anie.201102156.

(3) Labet, M.; Thielemans, W. Synthesis of Polycaprolactone: A Review. *Chem. Soc. Rev.* **2009**, *38* (12), 3484–3504. https://doi.org/10.1039/b820162p.

(4) Castro-Aguirre, E.; Iñiguez-Franco, F.; Samsudin, H.; Fang, X.; Auras, R. Poly(Lactic Acid)—Mass Production, Processing, Industrial Applications, and End of Life. *Adv. Drug Deliv. Rev.* **2016**, *107*, 333–366. https://doi.org/10.1016/j.addr.2016.03.010.

(5) Gupta, A. P.; Kumar, V. New Emerging Trends in Synthetic Biodegradable Polymers – Polylactide: A Critique. *Eur. Polym. J.* **2007**, *43* (10), 4053–4074. https://doi.org/10.1016/j.eurpolymj.2007.06.045.

(6) Dash, T. K.; Konkimalla, V. B. Poly(ϵ-Caprolactone) Based Formulations for Drug Delivery and Tissue Engineering: A Review. *J. Controlled Release* **2012**, *158* (1), 15–33. https://doi.org/10.1016/j.jconrel.2011.09.064.

(7) Kim, J. H.; Han, I. Biocompatible Hybrid Allyl 2-Cyanoacrylate and Hydroxyapatite Mixed for Bio-Glue. *J. Adhes. Sci. Technol.* **2017**, *31* (12), 1328–1337. https://doi.org/10.1080/01694243.2016.1256632.

(8) Martin, O.; Avérous, L. Poly(Lactic Acid): Plasticization and Properties of Biodegradable Multiphase Systems. *Polymer* **2001**, *42* (14), 6209–6219. https://doi.org/10.1016/S0032-3861(01)00086-6.

(9) Van de Velde, K.; Kiekens, P. Biopolymers: Overview of Several Properties and Consequences on Their Applications. *Polym. Test.* **2002**, *21* (4), 433–442. https://doi.org/10.1016/S0142-9418(01)00107-6.

(10) Becker, J. M.; Pounder, R. J.; Dove, A. P. Synthesis of Poly(Lactide)s with Modified Thermal and Mechanical Properties. *Macromol. Rapid Commun.* **2010**, *31* (22), 1923–1937. https://doi.org/10.1002/marc.201000088.

(11) Pitt, C. G.; Jeffcoat, A. R.; Zweidinger, R. A.; Schindler, A. Sustained Drug Delivery Systems. I. The Permeability of Poly(ε-Caprolactone), Poly(DL-Lactic Acid), and Their Copolymers. *J. Biomed. Mater. Res.* **1979**, *13* (3), 497–507. https://doi.org/10.1002/jbm.820130313.

(12) Pitt, C. G.; Chasalow, F. I.; Hibionada, Y. M.; Klimas, D. M.; Schindler, A. Aliphatic Polyesters. I. The Degradation of Poly(ϵ-Caprolactone) in Vivo. *J. Appl. Polym. Sci.* **1981**, *26* (11), 3779–3787. https://doi.org/10.1002/app.1981.070261124.

(13) Pitt, C. G.; Gratzl, M. M.; Kimmel, G. L.; Surles, J.; Schindler, A. Aliphatic Polyesters II. The Degradation of Poly (DL-Lactide), Poly (ε-Caprolactone), and Their Copolymers in Vivo. *Biomaterials* **1981**, *2* (4), 215–220. https://doi.org/10.1016/0142-9612(81)90060-0.

(14) Grijpma, D. W.; Zondervan, G. J.; Pennings, A. J. High Molecular Weight Copolymers of L-Lactide and ε-Caprolactone as Biodegradable Elastomeric Implant Materials. *Polym. Bull.* **1991**, *25* (3), 327–333. https://doi.org/10.1007/BF00316902.

(15) Jung, Y.; Park, M. S.; Lee, J. W.; Kim, Y. H.; Kim, S.-H.; Kim, S. H. Cartilage Regeneration with Highly-Elastic Three-Dimensional Scaffolds Prepared from Biodegradable Poly(L-Lactide-Co-ε-Caprolactone). *Biomaterials* **2008**, *29* (35), 4630–4636. https://doi.org/10.1016/j.biomaterials.2008.08.031.

(16) Lim, J. I.; Kim, S. il; Kim, S. H. Lotus-Leaf-like Structured Heparin-Conjugated Poly(L-Lactide-Co-ε-Caprolactone) as a Blood Compatible Material. *Colloids Surf. B Biointerfaces* **2013**, *103*, 463–467. https://doi.org/10.1016/j.colsurfb.2012.11.016.

(17) Cha, K. J.; Lih, E.; Choi, J.; Joung, Y. K.; Ahn, D. J.; Han, D. K. Shape-Memory Effect by Specific Biodegradable Polymer Blending for Biomedical Applications: Shape-Memory Effect by Specific Biodegradable Polymer. *Macromol. Biosci.* **2014**, *14* (5), 667–678. https://doi.org/10.1002/mabi.201300481.

(18) Kim, S. H.; Kim, S. H.; Jung, Y. TGF-β 3 Encapsulated PLCL Scaffold by a Supercritical CO 2 –HFIP Co-Solvent System for Cartilage Tissue Engineering. *J. Controlled Release* **2015**, *206*, 101–107. https://doi.org/10.1016/j.jconrel.2015.03.026.

(19) Calandrelli, L.; Calarco, A.; Laurienzo, P.; Malinconico, M.; Petillo, O.; Peluso, G. Compatibilized Polymer Blends Based on PDLLA and PCL for Application in Bioartificial Liver. **2008**, *9* (6), 1527–1534. https://doi.org/10.1021/bm7013087.

(20) Stirling, E.; Champouret, Y.; Visseaux, M. Catalytic Metal-Based Systems for Controlled Statistical Copolymerisation of Lactide with a Lactone. *Polym. Chem.* **2018**, *9* (19), 2517–2531. https://doi.org/10.1039/C8PY00310F.

(21) Lohmeijer, B. G. G.; Pratt, R. C.; Leibfarth, F.; Logan, J. W.; Long, D. A.; Dove, A. P.; Nederberg, F.; Choi, J.; Wade, C.; Waymouth, R. M.; et al. Guanidine and Amidine Organocatalysts for Ring-Opening Polymerization of Cyclic Esters. *Macromolecules* **2006**, *39* (25), 8574–8583. https://doi.org/10.1021/ma0619381.

(22) Alamri, H.; Zhao, J.; Pahovnik, D.; Hadjichristidis, N. Phosphazene-Catalyzed Ring-Opening Polymerization of ε-Caprolactone: Influence of Solvents and Initiators. *Polym Chem* **2014**, *5* (18), 5471–5478. https://doi.org/10.1039/C4PY00493K.

(23) Wang, Y.; Niu, J.; Jiang, L.; Niu, Y.; Zhang, L. Benzo-12-Crown-4 Modified N -Heterocyclic Carbene for Organocatalyst: Synthesis, Characterization and Degradation of Block Copolymers of ϵ-Caprolactone with *L* -Lactide. *J. Macromol. Sci. Part A* **2016**, *53* (6), 374–381. https://doi.org/10.1080/10601325.2016.1166004.

(24) Baśko, M.; Kubisa, P. Cationic Copolymerization of ε-Caprolactone and L,L-Lactide by an Activated Monomer Mechanism. *J. Polym. Sci. Part Polym. Chem.* **2006**, *44* (24), 7071–7081. https://doi.org/10.1002/pola.21712.

(25) Baśko, M.; Kubisa, P. Polyester Oligodiols by Cationic AM Copolymerization of L,L-Lactide and ε-Caprolactone Initiated by Diols. *J. Polym. Sci. Part Polym. Chem.* **2007**, *45* (14), 3090–3097. https://doi.org/10.1002/pola.22065.

(26) Zhou, X.; Hong, L. Controlled Ring-Opening Polymerization of Cyclic Esters with Phosphoric Acid as Catalysts. *Colloid Polym. Sci.* **2013**, *291* (9), 2155–2162. https://doi.org/10.1007/s00396-013-2950-9.

(27) Zhang, L.; Li, N.; Wang, Y.; Guo, J.; Li, J. Ring-Opening Block Copolymerization of ε-Caprolactone with L-Lactide Catalyzed by N-Heterocyclic Carbenes: Synthesis,

Characteristics, Mechanism. *Macromol. Res.* **2014**, *22* (6), 600–605. https://doi.org/10.1007/s13233-014-2092-z.

(28) Pothupitiya, J. U.; Dharmaratne, N. U.; Jouaneh, T. M. M.; Fastnacht, K. V.; Coderre, D. N.; Kiesewetter, M. K. H-Bonding Organocatalysts for the Living, Solvent-Free Ring-Opening Polymerization of Lactones: Toward an All-Lactones, All-Conditions Approach. *Macromolecules* **2017**, *50* (22), 8948–8954. https://doi.org/10.1021/acs.macromol.7b01991.

(29) Mezzasalma, L.; De Winter, J.; Taton, D.; Coulembier, O. Extending the Scope of Benign and Thermally Stable Organocatalysts: Application of Dibenzoylmethane for the Bulk Copolymerization of L-Lactide and ε-Caprolactone. *J. Polym. Sci. Part Polym. Chem.* **2018**, *56* (5), 475–479. https://doi.org/10.1002/pola.28921.

(30) Song, Q.; Hu, S.; Zhao, J.; Zhang, G. Organocatalytic Copolymerization of Mixed Type Monomers. *Chin. J. Polym. Sci.* **2017**, *35* (5), 581–601. https://doi.org/10.1007/s10118-017-1925-6.

(31) Grijpma, D. W.; Pennings, A. J. Polymerization Temperature Effects on the Properties of L-Lactide and ε-Caprolactone Copolymers. *Polym. Bull.* **1991**, *25* (3), 335–341. https://doi.org/10.1007/BF00316903.

(32) Vanhoorne, P.; Dubois, P.; Jerome, R.; Teyssie, P. Macromolecular Engineering of Polylactones and Polylactides. 7. Structural Analysis of Copolyesters of ε-Caprolactone and L- or D,L-Lactide Initiated by Triisopropoxyaluminum. *Macromolecules* **1992**, *25* (1), 37–44. https://doi.org/10.1021/ma00027a008.

(33) Shen, Y.; Zhu, K. J.; Shen, Z.; Yao, K.-M. Synthesis and Characterization of Highly Random Copolymer of ϵ-Caprolactone and D,L-Lactide Using Rare Earth Catalyst. *J. Polym. Sci. Part Polym. Chem.* **1996**, *34* (9), 1799–1805. https://doi.org/10.1002/(SICI)1099-0518(19960715)34:9<1799::AID-POLA18>3.0.CO;2-1.

(34) Contreras, J.; Dávila, D. Ring-Opening Copolymerization of L-Lactide with ε-Caprolactone Initiated by Diphenylzinc. *Polym. Int.* **2006**, *55* (9), 1049–1056. https://doi.org/10.1002/pi.2050.

(35) Florczak, M.; Duda, A. Effect of the Configuration of the Active Center on Comonomer Reactivities: The Case of ε-Caprolactone/L,L-Lactide Copolymerization. *Angew. Chem. Int. Ed.* **2008**, *47* (47), 9088–9091. https://doi.org/10.1002/anie.200803540.

(36) Pappalardo, D.; Annunziata, L.; Pellecchia, C. Living Ring-Opening Homo- and Copolymerization of ε-Caprolactone and L,L-Lactides by Dimethyl(Salicylaldiminato)Aluminum Compounds. *Macromolecules* **2009**, *42* (16), 6056–6062. https://doi.org/10.1021/ma9010439.

(37) Wei, Z.; Liu, L.; Qu, C.; Qi, M. Microstructure Analysis and Thermal Properties of L-Lactide/ε-Caprolactone Copolymers Obtained with Magnesium Octoate. *Polymer* **2009**, *50* (6), 1423–1429. https://doi.org/10.1016/j.polymer.2009.01.015.

(38) Nomura, N.; Akita, A.; Ishii, R.; Mizuno, M. Random Copolymerization of ε-Caprolactone with Lactide Using a Homosalen−Al Complex. *J. Am. Chem. Soc.* **2010**, *132* (6), 1750–1751. https://doi.org/10.1021/ja9089395.

(39) Li, G.; Lamberti, M.; Pappalardo, D.; Pellecchia, C. Random Copolymerization of ε-Caprolactone and Lactides Promoted by Pyrrolylpyridylamido Aluminum Complexes. *Macromolecules* **2012**, *45* (21), 8614–8620. https://doi.org/10.1021/ma3019848.

(40) Shi, T.; Luo, W.; Liu, S.; Li, Z. Controlled Random Copolymerization of Rac-Lactide and ε-Caprolactone by Well-Designed Phenoxyimine Al Complexes. *J. Polym. Sci. Part Polym. Chem.* **2018**, *56* (6), 611–617. https://doi.org/10.1002/pola.28932.

(41) Honrado, M.; Otero, A.; Fernández-Baeza, J.; Sánchez-Barba, L. F.; Garcés, A.; Lara-Sánchez, A.; Rodríguez, A. M. Copolymerization of Cyclic Esters Controlled by Chiral NNO-Scorpionate Zinc Initiators. *Organometallics* **2016**, *35* (2), 189–197. https://doi.org/10.1021/acs.organomet.5b00919.

(42) Maruta, Y.; Abiko, A. Random Copolymerization of ε-Caprolactone and L-Lactide with Molybdenum Complexes. *Polym. Bull.* **2014**, *71* (4), 989–999. https://doi.org/10.1007/s00289-014-1106-5.

(43) Nachtergael, A.; Coulembier, O.; Dubois, P.; Helvenstein, M.; Duez, P.; Blankert, B.; Mespouille, L. Organocatalysis Paradigm Revisited: Are Metal-Free Catalysts Really Harmless? **2015**, *16* (2), 507–514. https://doi.org/10.1021/bm5015443.

(44) Dove, A. P. Organic Catalysis for Ring-Opening Polymerization. *ACS Macro Lett.* **2012**, *1* (12), 1409–1412. https://doi.org/10.1021/mz3005956.

(45) Kiesewetter, M. K.; Shin, E. J.; Hedrick, J. L.; Waymouth, R. M. Organocatalysis: Opportunities and Challenges for Polymer Synthesis. *Macromolecules* **2010**, *43* (5), 2093–2107. https://doi.org/10.1021/ma9025948.

(46) Kamber, N. E.; Jeong, W.; Waymouth, R. M.; Pratt, R. C.; Lohmeijer, B. G. G.; Hedrick, J. L. Organocatalytic Ring-Opening Polymerization. *Chem. Rev.* **2007**, *107* (12), 5813–5840. https://doi.org/10.1021/cr068415b.

(47) Fèvre, M.; Pinaud, J.; Gnanou, Y.; Vignolle, J.; Taton, D. N-Heterocyclic Carbenes (NHCs) as Organocatalysts and Structural Components in Metal-Free Polymer Synthesis. *Chem. Soc. Rev.* **2013**, *42* (5), 2142–2172. https://doi.org/10.1039/c2cs35383k.

(48) Thomas, C.; Bibal, B. Hydrogen-Bonding Organocatalysts for Ring-Opening Polymerization. *Green Chem* **2014**, *16* (4), 1687–1699. https://doi.org/10.1039/C3GC41806E.

(49) Ottou, W. N.; Sardon, H.; Mecerreyes, D.; Vignolle, J.; Taton, D. Update and Challenges in Organo-Mediated Polymerization Reactions. *Prog. Polym. Sci.* **2016**, *56*, 64–115. https://doi.org/10.1016/j.progpolymsci.2015.12.001.

(50) Naumann, S.; Dove, A. P. N-Heterocyclic Carbenes for Metal-Free Polymerization Catalysis: An Update: N-Heterocyclic Carbenes for Metal-Free Polymerization Catalysis. *Polym. Int.* **2016**, *65* (1), 16–27. https://doi.org/10.1002/pi.5034.

(51) Lindquist, E.; Yang, Y. Degradation of Benzoic Acid and Its Derivatives in Subcritical Water. *J. Chromatogr. A* **2011**, *1218* (15), 2146–2152. https://doi.org/10.1016/j.chroma.2010.08.054.

(52) Mezzasalma, L.; De Winter, J.; Taton, D.; Coulembier, O. Benzoic Acid-Organocatalyzed Ring-Opening (Co)Polymerization (ORO(c)P) of L-Lactide and ε-Caprolactone under Solvent-Free Conditions: From Simplicity to Recyclability. *Green Chem.* **2018**, *20* (23), 5385–5396. https://doi.org/10.1039/C8GC03096K.

(53) Van Den Brink, M.; Van Herk, A. M.; German, A. L. Nonlinear Regression by Visualization of the Sum of Residual Space Applied to the Integrated Copolymerization Equation with Errors in All Variables. I. Introduction of the Model, Simulations and Design of Experiments. *J. Polym. Sci. Part Polym. Chem.* **1999**, *37* (20), 3793–3803. https://doi.org/10.1002/(SICI)1099-0518(19991015)37:20<3793::AID-POLA8>3.0.CO;2-Q.

(54) Harrisson, S.; Ercole, F.; Muir, B. W. Living Spontaneous Gradient Copolymers of Acrylic Acid and Styrene: One-Pot Synthesis of PH-Responsive Amphiphiles. *Polym Chem* **2010**, *1* (3), 326–332. https://doi.org/10.1039/B9PY00301K.

(55) Stilbs, P. Molecular Self-Diffusion Coefficients in Fourier Transform Nuclear Magnetic Resonance Spectrometric Analysis of Complex Mixtures. *Anal. Chem.* **1981**, *53* (13), 2135–2137. https://doi.org/10.1021/ac00236a044.

(56) Johnson, C. S. Diffusion Ordered Nuclear Magnetic Resonance Spectroscopy: Principles and Applications. *Prog. Nucl. Magn. Reson. Spectrosc.* **1999**, *34* (3–4), 203–256. https://doi.org/10.1016/S0079-6565(99)00003-5.

(57) Longsworth, L. G. The Mutual Diffusion of Light and Heavy Water. *J. Phys. Chem.* **1960**, *64* (12), 1914–1917. https://doi.org/10.1021/j100841a027.

(58) Holz, M.; Weingartner, H. Calibration in Accurate Spin-Echo Self-Diffusion Measurements Using 1H and Less-Common Nuclei. *J. Magn. Reson. 1969* **1991**, *92* (1), 115–125. https://doi.org/10.1016/0022-2364(91)90252-O.

(59) Coulembier, O.; Moins, S.; Raquez, J.-M.; Meyer, F.; Mespouille, L.; Duquesne, E.; Dubois, P. Thermal Degradation of Poly(L-Lactide): Accelerating Effect of Residual DBU-Based Organic Catalysts. *Polym. Degrad. Stab.* **2011**, *96* (5), 739–744. https://doi.org/10.1016/j.polymdegradstab.2011.02.014.

(60) Fan, Y.; Nishida, H.; Shirai, Y.; Tokiwa, Y.; Endo, T. Thermal Degradation Behaviour of Poly(Lactic Acid) Stereocomplex. *Polym. Degrad. Stab.* **2004**, *86* (2), 197–208. https://doi.org/10.1016/j.polymdegradstab.2004.03.001.

(61) Mayo, F. R.; Lewis, F. M. Copolymerization. I. A Basis for Comparing the Behavior of Monomers in Copolymerization; The Copolymerization of Styrene and Methyl Methacrylate. *J. Am. Chem. Soc.* **1944**, *66* (9), 1594–1601. https://doi.org/10.1021/ja01237a052.

(62) Kasperczyk, J.; Bero, M. Coordination Polymerization of Lactides, 2. Microstructure Determination of Poly[(L,L-Lactide)-Co-(ε-Caprolactone)] with 13C Nuclear Magnetic Resonance Spectroscopy. *Makromol. Chem.* **1991**, *192* (8), 1777–1787. https://doi.org/10.1002/macp.1991.021920812.

(63) Kasperczyk, J.; Bero, M. Coordination Polymerization of Lactides, 4. The Role of Transesterification in the Copolymerization of L,L-Lactide and ε-Caprolactone. *Makromol. Chem.* **1993**, *194* (3), 913–925. https://doi.org/10.1002/macp.1993.021940315.

(64) Xia, Y.; Shen, J.; Alamri, H.; Hadjichristidis, N.; Zhao, J.; Wang, Y.; Zhang, G. Revealing the Cytotoxicity of Residues of Phosphazene Catalysts Used for the Synthesis of Poly(Ethylene Oxide). **2017**, *18* (10), 3233–3237. https://doi.org/10.1021/acs.biomac.7b00891.

(65) Dubois-Pot-Schneider, H.; Fekir, K.; Coulouarn, C.; Glaise, D.; Aninat, C.; Jarnouen, K.; Le Guével, R.; Kubo, T.; Ishida, S.; Morel, F.; et al. Inflammatory Cytokines Promote the Retrodifferentiation of Tumor-Derived Hepatocyte-like Cells to Progenitor Cells: HEPATOLOGY, Vol. 00, No. X, 2014. *Hepatology* **2014**, *60* (6), 2077–2090. https://doi.org/10.1002/hep.27353.

(66) Cerec, V.; Glaise, D.; Garnier, D.; Morosan, S.; Turlin, B.; Drenou, B.; Gripon, P.; Kremsdorf, D.; Guguen-Guillouzo, C.; Corlu, A. Transdifferentiation of Hepatocyte-like Cells from the Human Hepatoma HepaRG Cell Line through Bipotent Progenitor. *Hepatology* **2007**, *45* (4), 957–967. https://doi.org/10.1002/hep.21536.

(67) Aninat, C.; Piton, A.; Glaise, D.; Le Charpentier, T.; Langouët, S.; Morel, F.; Guguen-Guillouzo, C.; Guillouzo, A. Expression Of Cytochromes P450, Conjugating Enzymes And Nuclear Receptors In Human Hepatoma Heparg Cells. *Drug Metab. Dispos.* **2005**, *34* (1), 75–83. https://doi.org/10.1124/dmd.105.006759.

(68) Quesnot, N.; Bucher, S.; Gade, C.; Vlach, M.; Vene, E.; Valença, S.; Gicquel, T.; Holst, H.; Robin, M.-A.; Loyer, P. Production of Chlorzoxazone Glucuronides via Cytochrome P4502E1 Dependent and Independent Pathways in Human Hepatocytes. *Arch. Toxicol.* **2018**, *92* (10), 3077–3091. https://doi.org/10.1007/s00204-018-2300-2.

(69) Josse, R.; Aninat, C.; Glaise, D.; Dumont, J.; Fessard, V.; Morel, F.; Poul, J.-M.; Guguen-Guillouzo, C.; Guillouzo, A. Long-Term Functional Stability of Human HepaRG Hepatocytes and Use for Chronic Toxicity and Genotoxicity Studies. *Drug Metab. Dispos.* **2008**, *36* (6), 1111–1118. https://doi.org/10.1124/dmd.107.019901.

(70) Quesnot, N.; Rondel, K.; Audebert, M.; Martinais, S.; Glaise, D.; Morel, F.; Loyer, P.; Robin, M.-A. Evaluation of Genotoxicity Using Automated Detection of ΓH2AX in Metabolically Competent HepaRG Cells. *Mutagenesis* **2015**, gev059. https://doi.org/10.1093/mutage/gev059.

Bulk Organocatalytic Synthetic Access to Statistical Copolyesters from L-Lactide and ε-Caprolactone Using Benzoic Acid

Leila Mezzasalma, Simon Harrisson,* Saad Saba, Pascal Loyer, Olivier Coulembier,* and Daniel Taton*

Use for table of content only: